

MgO Nanostructures on Au(111) as Catalysts for Low-Temperature Methane Activation and C–C Coupling

Arephin Islam, Pedro J. Ramírez, Kasala Prabhakar Reddy, Irene Barba-Nieto, Adrian Hunt, Iradwikanari Waluyo, and José A. Rodríguez*



Cite This: *J. Phys. Chem. Lett.* 2025, 16, 7600–7604



Read Online

ACCESS |



Metrics & More

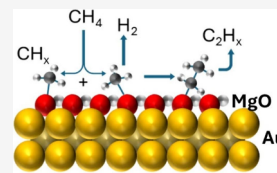


Article Recommendations



Supporting Information

ABSTRACT: The selective conversion of methane (CH_4) under mild conditions remains challenging due to strong C–H bonds and catalyst coking. We systematically investigated submonolayer MgO nanostructures on Au(111), where two-dimensional (2D) MgO islands with stable Mg–O–Au interfaces catalyze low-temperature CH_4 activation and C–C coupling. Upon CH_4 exposure at 300 K, surface-bound CH_x and C_2H_x intermediates formed and persisted postevacuation, indicating robust CH_x –O–Mg linkages. Temperature-programmed studies revealed that C–H activation and C–C coupling intensify with heat: the CH_x signal grew continuously while the C_2H_x signal reached a plateau at 400–500 K. O 1s and Mg 2p attenuation confirmed adsorption of the hydrocarbons on MgO. Catalytic tests at 500 K yielded C_2H_6 (70%) and C_2H_4 (30%) without coking, underscoring MgO's role as an active catalyst. These results offer new design principles for developing coke-resistant and low-temperature methane upgrading catalysts.



The direct conversion of methane (CH_4) into higher alkanes or olefins represents a highly attractive yet challenging process due to the intrinsic difficulty of activating CH_4 . Alkaline earth metals (Be, Mg, Ca, Sr, Ba) have traditionally been used as promoters,^{1–4} which influence surface reaction rates through electronic interactions, surface reconstruction, or direct bonding with adsorbates rather than serving as active catalytic centers.^{5,6} However, their effectiveness is highly dependent on surface coverage; excessive coverage can lead to charge redistribution effects that deactivate the catalyst by excessive charge transfer. Among various alkaline earth metals, Mg-based systems have garnered significant attention due to their tunable basicity, stability, and potential to activate CH_4 .^{1–4}

Since the 1990s, a lot of attention has been focused on the activation of CH_4 and subsequent C–C coupling to yield ethane (C_2H_6) and ethylene (C_2H_4) on bulk magnesium oxide (MgO).^{7,8} The process is challenging because CH_4 activation involves the breaking of stable C–H bonds (bond dissociation energy: 460 kJ/mol).⁹ On bulk MgO, the $\text{CH}_{4,\text{gas}} \rightarrow \text{CH}_{x,\text{ads}} + (4-x)\text{H}_{\text{ads}}$ reaction takes place at high reaction temperatures, typically exceeding 700 K.¹⁰ These harsh conditions not only elevate energy consumption but also promote rapid catalyst deactivation due to carbon deposition (coking), which blocks active sites. Strategies to overcome these limitations include doping MgO with transition metals, such as Ni, or alkali elements, such as Li, to create metal/oxide interfaces that enhance catalytic reactivity.^{7,8,10} Another promising approach is the deposition of MgO as nanostructures on metal surfaces, which modifies the oxide electronic properties and facilitates charge transfer, improving catalytic efficiency.^{11,12} Recent studies have demonstrated that MgO nanostructures (<1 nm) supported on $\text{Cu}_2\text{O}/\text{Cu}(111)$ surfaces exhibit unique

reactivity toward CH_4 , dissociating it into reactive intermediates such as CH_x and hydrogen adatoms.¹² Notably, these nanostructures enable C–C coupling into ethane and ethylene at 500 K — a significantly lower temperature than required for bulk MgO catalysts (>700 K).¹⁰ This process occurs with minimal carbon deposition, preventing deactivation. Density functional theory (DFT) calculations corroborated these findings, indicating that CH_4 dissociation is energetically favorable on $\text{MgO}/\text{Cu}_2\text{O}/\text{Cu}(111)$ surfaces.¹² Thus, the Mg–O–Cu interface was active in the conversion of CH_4 , and a key question is what would happen if Cu were replaced by a much less reactive metal? What is the intrinsic activity of MgO nanostructures in methane coupling? In this study, we investigated the chemical behavior of MgO nanostructures on an inert Au(111) substrate.

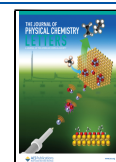
The structural and electronic properties of MgO overlayers have been investigated on Au(111) in previous works.^{13–16} Different growth modes were observed for the MgO islands with scanning tunneling microscopy (STM).^{1,2} Depending on the deposition temperature and oxygen partial pressure, either compact MgO patches with a (001) lattice configuration or triangular/hexagonal islands with a (111) lattice were found.^{13,15} The MgO grew on the gold substrate forming two or three-dimensional (2D or 3D) islands.^{15,16} The results of density functional calculations showed that the structural

Received: May 14, 2025

Revised: July 11, 2025

Accepted: July 15, 2025

Published: July 21, 2025



and electronic properties of the island were strongly influenced by interactions with the underlying metal.¹⁶ Upon deposition on Au(111), MgO undergoes substantial electronic modification, including a reduction in the work function and an upward shift of the Shockley surface state of gold due to interfacial charge transfer and lattice mismatch effects.^{13–16} Scanning tunneling microscopy and spectroscopy studies reveal the formation of a (6×1) superlattice due to lattice mismatch between hexagonal Au(111) and square MgO(001), significantly influencing electron transport.¹³ Additionally, field-emission resonance shifts and interface dipole formation indicate strong charge-transfer effects at the MgO/Au interface.¹³ These modifications can profoundly impact catalytic performance by altering adsorption energies and reaction selectivity, making a study of CH₄ activation on MgO nanostructures dispersed on Au(111) interesting from scientific and practical viewpoints.

Figures S1 and S2 display AP-XPS spectra (Au 4f, Mg 2p, and O 1s regions) collected for gold surfaces with 0.08 and 0.15 ML of MgO_x. The Au 4f spectra exhibit two distinct doublets corresponding to surface Au⁰ (83.7 eV for the 4f_{7/2} peak) and bulk Au⁰ (84 eV for the 4f_{7/2} peak).¹⁷ The deposition of the low amounts of MgO_x produced a very small decrease in the 4f features for the Au surface atoms. The Mg was vapor-deposited onto the gold under a background pressure of 1×10^{-6} Torr O₂ at 300 K, followed by post-treatment in 50 mTorr of O₂ at 500 K for 30 min. Following this oxidation treatment, the Mg 2p binding energy appeared near the value of 49.5 eV expected for MgO nanostructures.^{11,12}

Figure 1 compares the O 1s spectra for the two coverages of MgO on Au(111). Peaks can be observed near 529 and 531 eV. The peak at higher binding energy corresponds to O atoms in MgO nanostructures,^{11,12} while the peak at lower energy

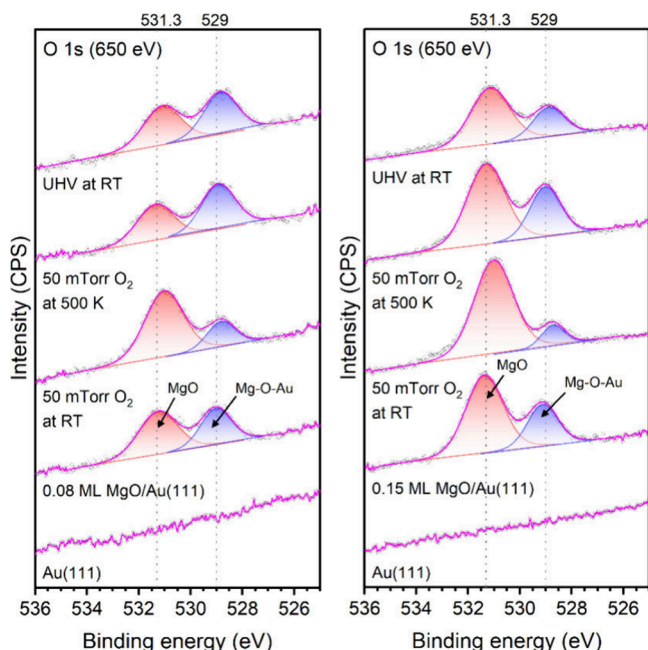


Figure 1. O 1s AP-XPS spectra for pristine Au(111) and for surfaces with 0.08 (left panel) and 0.15 ML (right panel) of MgO_x. The Mg was vapor-deposited on the Au(111) substrate under a background of 1×10^{-6} Torr of O₂ at 300 K. Then, the systems were treated with 50 mTorr of O₂ at 500 K for 30 min.

comes from O atoms bound to Au or present in a Mg–O–Au interface.^{18,19} Atomic O can be deposited on Au(111) by decomposing ozone and has an O 1s binding energy of 529–530 eV.^{18,19} Since O₂ does not dissociate on Au(111),^{18,19} the O present on Au or the Mg–O–Au interface probably migrated from the MgO nanostructures. As shown in Figure S3, temperature had a strong effect on the relative intensity of the oxygen features. When the temperature increased from 300 to 500 K, O atoms migrated from the MgO nanostructures and the intensity of the Mg–O–Au features grew. In contrast the dosing of O₂, as shown in Figure 1, increased the amount of MgO present on the Au(111) substrate. An analysis of the peak intensities in Figure 1 points to a dynamic system where the composition depends on the temperature and chemical environment around the sample (Figure S4).

Previous studies have shown that MgO can grow on Au(111) forming 2D or 3D islands.^{13–16} Results of ion scattering spectroscopy (ISS) in Figure S5 indicate that the low MgO_x coverages examined in Figures 1, S1 and S2 correspond to 2D islands. At higher oxide coverages (>0.2 ML), 3D growth occurs (Figure S3). In the next two sections, we will focus our attention mainly on the chemical and catalytic properties of small 2D coverages of MgO_x (<0.2 ML), which interact strongly with the gold substrate and exhibit unique electronic and structural properties.^{13–16}

We found no adsorption of methane on clean Au(111). Also, there was no methane binding on O/Au(111). Figures 2,

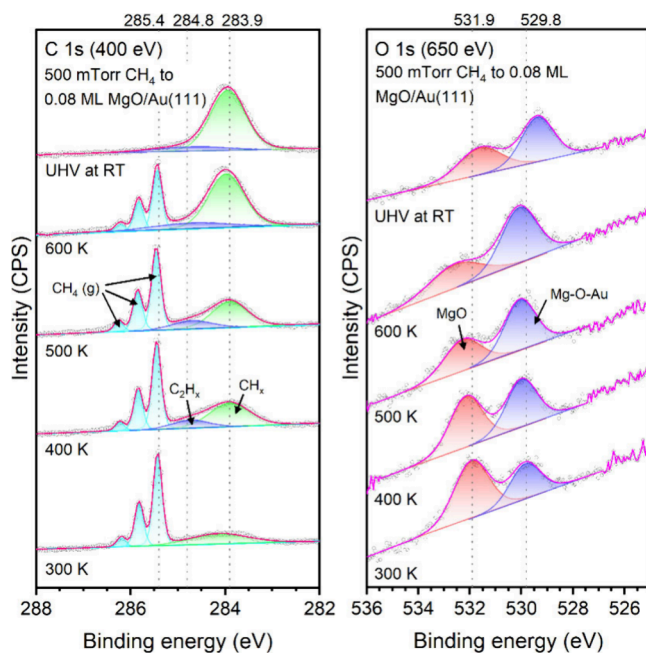


Figure 2. C 1s and O 1s AP-XPS spectra collected while exposing a MgO_x/Au(111) surface with 0.08 ML of Mg to 500 mTorr CH₄ between 300 and 600 K. In preliminary steps, the surface was exposed to 50 mTorr of O₂ at 500 K, see Figure S4.

S6 and S7 show a set of AP-XPS spectra collected while exposing a Au(111) surface with 0.08 ML of MgO_x to methane at temperatures between 300 and 600 K. This MgO_x/Au(111) system was able to carry out the CH_{4,gas} → CH_{x,ads} + (4 – x)H_{ads} reaction at room temperature. A trace of adsorbed CH_x (at 283.9 eV)¹² was detected after exposing the system to 10^{-6}

Torr of methane at 300 K (Figure S4), and the signal for this surface intermediate raised when the CH_4 pressure was increased to 500 mTorr. Notably, the CH_x signal persisted after evacuation at 300 K (Figure S6), opening the possibility of C–C coupling on the $\text{MgO}_x/\text{Au}(111)$ surface.

In Figure 2, the amount of adsorbed CH_x substantially increases when the temperature of the sample is increased from 300 to 600 K under a CH_4 constant pressure of 500 mTorr. At temperatures of 400 K and above, the C 1s spectra not only show the presence of CH_x species at 283.9 eV but also exhibit an additional peak at 284.8 eV, which can be attributed to C_2H_x species^{12,20,21} generated by C–C coupling. No signal was observed in the 283–282 eV region where atomic C appears.^{12,20,21} In the corresponding O 1s spectra, the relative intensity of the MgO features decreases after the generation of $\text{CH}_x/\text{C}_2\text{H}_x$ on the surface. At the end, they are significantly smaller than in the presence of O_2 gas (Figure 1). There was also a positive binding energy shift (0.4–0.8 eV) in the Mg 2p features (Figures S6 and S7). Thus, the XPS data suggest that the $\text{CH}_x/\text{C}_2\text{H}_x$ species are mainly bound on top of the MgO. This is consistent with our previous finding that methane does not adsorb on $\text{O}/\text{Au}(111)$ or $\text{Au}(111)$.

Figures 3, S8 and S9 display AP-XPS spectra recorded while exposing a $\text{Au}(111)$ surface with 0.15 ML of MgO_x to methane

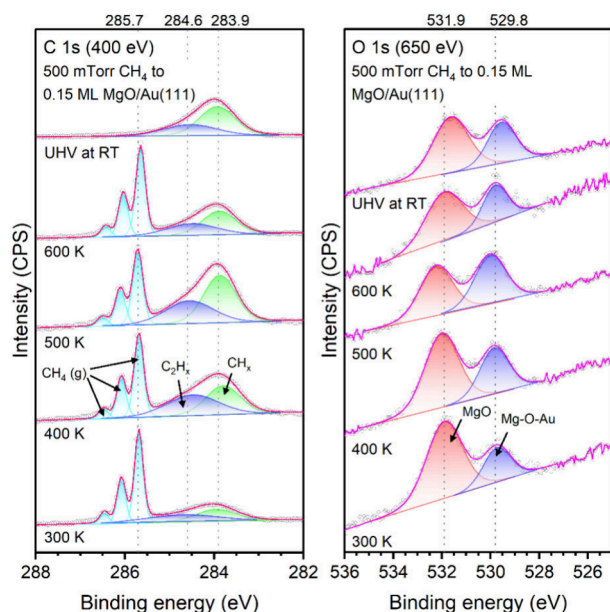


Figure 3. C 1s and O 1s AP-XPS spectra collected while exposing a $\text{MgO}_x/\text{Au}(111)$ surface with 0.15 ML of Mg to 500 mTorr of CH_4 between 300 and 600 K. In preliminary steps, the surface was exposed to 50 mTorr of O_2 at 500 K, see Figure 1, and then to CH_4 at 300 K, see Figure S6.

at temperatures between 300 and 600 K. Again, the $\text{MgO}_x/\text{Au}(111)$ surface was able to activate methane at room temperature and a CH_4 pressure of 1×10^{-6} Torr (Figure S8). The formation of C_2H_x (at ~ 284.6 eV)^{12,20,21} appears now at 300 K and the signal clearly grows until 500 K (Figure 3). No signal is seen for atomic C (283–282 eV).^{20,21} In the O 1s region, the attenuation of the signal for MgO points to preferential adsorption of $\text{CH}_x/\text{C}_2\text{H}_x$ on the oxide component. Indeed, at 500 K, the $\text{MgO}/\text{Mg-O-Au}$ ratio obtained from the O 1s spectra tracks the formation of $\text{CH}_x/\text{C}_2\text{H}_x$ (Figure S10).

Figure 4 compares the concentration of CH_x and C_2H_x species on the $\text{MgO}_x/\text{Au}(111)$ surfaces as a function of

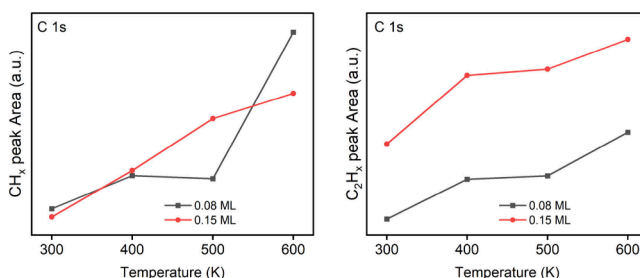


Figure 4. Relative peak areas for CH_x and C_2H_x species adsorbed on $\text{Au}(111)$ surfaces with 0.08 (Figure 2) and 0.15 ML (Figure 3) of MgO as a function of temperature under 500 mTorr of methane. The peak areas were normalized with respect to the gas phase CH_4 peaks obtained from Figures 2 and 3.

temperature. Both coverages display high activity for CH_x generation at 400 and 500 K. The presence of C_2H_x adsorbates highlights a unique reactivity of the $\text{MgO}_x/\text{Au}(111)$ system at higher coverage, suggesting that larger or more interconnected MgO domains provide favorable sites for coupling reactions beyond simple C–H bond activation.

We also investigated the reaction of CH_4 with $\text{MgO}_x/\text{Au}(111)$ surfaces that had medium and large oxide coverages (>0.15 ML, Figure S9). In these systems, the MgO_x was growing forming 3D islands (Figure S5), they were more active than plain $\text{Au}(111)$, but their ability to dissociate methane decreased very fast when the oxide coverage increased (Figure S11). The oxide overlayer was moving toward the chemical properties of bulk MgO that only dissociates methane at temperatures above 700 K.¹⁰

$\text{Au}(111)$ and $\text{O}/\text{Au}(111)$ were inactive as catalysts for methane coupling. In contrast, catalytic tests showed that the $\text{MgO}_x/\text{Au}(111)$ surfaces were able to perform C–C coupling to generate C_2H_6 and C_2H_4 (Figures 5 and S12). The best performance as a catalyst was seen for a system with 0.15 ML of MgO_x , which also displayed the highest ability to dissociate methane (Figure S11). We only detected C_2H_6 ($\sim 70\%$ selectivity) and C_2H_4 ($\sim 30\%$ selectivity) as the hydrocarbon products of CH_4 coupling. Since most of the $\text{CH}_x/\text{C}_2\text{H}_x$ species were bound to the MgO nanoparticles (see above), it is valid to assume that these are also the active sites for catalytic C–C coupling. Assuming that all the Mg cations in a $\text{MgO}_x/\text{Au}(111)$ surface are chemically active, we estimated turnover numbers (TONs) of 0.21 molecules/s for the production of C_2H_6 and 0.09 molecules/s for the production of C_2H_4 on the catalysts with 0.15 ML of MgO_x . Compared to other catalysts for methane coupling reported in the literature,^{7,8,10} our system is very competitive in terms of yield and a relatively low temperature of operation. The 0.15 ML $\text{MgO}_x/\text{Au}(111)$ catalyst has an activity at a temperature that is comparable to that reported for a Pt/SiO_2 catalyst (520 K),²² but our system is stable with time (Figure 5a and S12) and does not deactivate by rapid coke deposition as seen for Pt/SiO_2 ²² and catalysts containing bulk MgO.^{7,8,10} After several cycles of continuous operation for 3 h (Figure S12), we saw no signs of catalyst deactivation and the coverage of C/ CH_x species remained very low (<0.15 ML after 18 h of operation). In Figure 3, the C 1s AP-XPS spectra show that the coverage of carbon (expected at 283–282 eV)^{20,21,23} generated

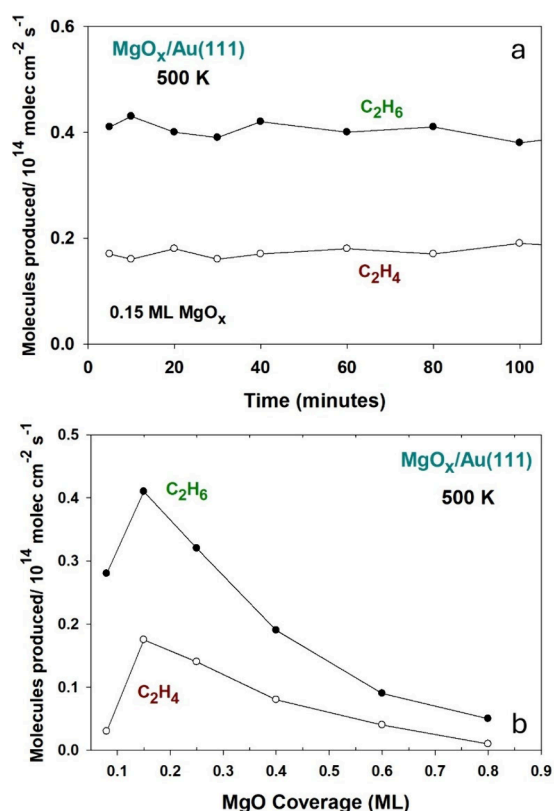


Figure 5. (a) Production of ethane (C₂H₆) and ethylene (C₂H₄) through methane coupling on a 0.15 ML MgO_x/Au(111) surface exposed to 5 Torr of CH₄ at 500 K. (b) Effect of the MgO_x coverage on the production of C₂H₆ and C₂H₄.

on the MgO_x/Au(111) system at 300–500 K was negligible, in agreement with the findings of postreaction characterization with XPS (see Figures S11a and S12) for the catalyst in Figure 5. Thus, our system does not undergo deactivation due to carbon deposition or coke formation as seen for Pt/SiO₂ and catalysts based on bulk MgO.

In Figure 5b, the reduction in catalytic activity seen when the MgO_x coverage increases matches well the drop observed for the activation of CH₄ (Figure S11) and probably reflects the formation of 3D islands of MgO_x on the gold substrate (Figure S5). The 2D islands of MgO_x are the ones that exhibit the largest structural and electronic perturbations in the supported oxide,^{13–16} and these are probably responsible for the high chemical and catalytic activity seen in Figures 2, 3 and 5. A charge transfer from the Au substrate through the MgO overlayer is known to facilitate the bonding of adsorbates such as CO, water or O₂,^{24,25} and probably enhances the reactivity of the oxide toward methane as seen for MgO_x/Cu(111).¹²

The efficient conversion of methane (the main component in natural gas) into valuable hydrocarbons is crucial for advancing sustainable energy solutions. In a previous work, we found that MgO nanostructures embedded on a CuO_x/Cu(111) substrate were able to activate methane at low temperatures.¹² It was not clear if the activation of the alkane was done on top of the embedded MgO or on the Mg–O–Cu interface. On an inert Au(111) substrate, the AP-XPS results in Figures 2 and 3 point to a direct role of the MgO nanostructures in the activation of methane. Our results show that these oxide nanostructures do not need to be associated with a metal with a high chemical activity.

Interestingly, the selectivity for the yield of a high-value product like ethylene on MgO_x/Au(111) was 2–3 times larger than seen on MgO_x/CuO_x/Cu(111).¹² For the medium temperature of 500 K tested in Figure 5a, the TON for the production of C₂H₄ was 0.09 molecules/s on MgO_x/Au(111), while a value of 0.05 molecules/s was measured on MgO_x/CuO_x/Cu(111).¹² Due to their low cost and high catalytic performance, the MgO nanostructures deserve special attention when the goal is to transform methane into high value chemicals.

In summary, our ambient-pressure XPS study reveals that MgO_x—an oxide of an alkaline earth metal—functions as an active catalyst center rather than a mere promoter, with 2D islands supported on Au(111) effectively activating methane at room temperature and enabling C–C coupling to produce C₂H₆ and C₂H₄ at a relatively low temperature of 500 K. At 300 K, CH_x intermediates readily form on terminal oxide sites and persist after gas evacuation, while C₂H_x species emerge at higher MgO coverages, pointing to surface C–C bond formation without catastrophic coking. Heating from 300 to 600 K under CH₄ further enhances both C–H dissociation and C–C coupling. The observed behavior of MgO_x/Au(111) surfaces highlights the critical roles of oxide–metal interfacial chemistry, nanostructure morphology, and reaction temperature in controlling low-temperature methane activation and coupling, thereby offering clear design principles for developing coke-resistant and efficient catalysts for selective upgrading of methane under mild conditions.

■ ASSOCIATED CONTENT

Supporting Information

The Supporting Information is available free of charge at <https://pubs.acs.org/doi/10.1021/acs.jpclett.5c01471>.

Experimental details and AP-XPS and ISS results for the characterization of MgO_x/Au(111) surfaces under vacuum or O₂ or CH₄ atmospheres (PDF)

■ AUTHOR INFORMATION

Corresponding Author

José A. Rodríguez — Chemistry Division, Brookhaven National Laboratory, Upton, New York 11973, United States; orcid.org/0000-0002-5680-4214; Phone: 631-344-2246; Email: rodriguez@bnl.gov

Authors

Arephin Islam — Chemistry Division, Brookhaven National Laboratory, Upton, New York 11973, United States; orcid.org/0000-0001-8528-859X

Pedro J. Ramírez — Facultad de Ciencias, Universidad Central de Venezuela, Caracas 1020-A, Venezuela; Zoneca-CENEX, R&D Laboratories, 64770 Monterrey, México

Kasala Prabhakar Reddy — Chemistry Division, Brookhaven National Laboratory, Upton, New York 11973, United States; orcid.org/0000-0002-1616-5374

Irene Barba-Nieto — Chemistry Division, Brookhaven National Laboratory, Upton, New York 11973, United States; orcid.org/0000-0001-7793-685X

Adrian Hunt — National Synchrotron Light Source II, Brookhaven National Laboratory, Upton, New York 11973, United States; orcid.org/0000-0002-5283-9647

Iradwikanari Waluyo – National Synchrotron Light Source II, Brookhaven National Laboratory, Upton, New York 11973, United States; orcid.org/0000-0002-4046-9722

Complete contact information is available at:
<https://pubs.acs.org/10.1021/acs.jpclett.5c01471>

Notes

The authors declare no competing financial interest.

ACKNOWLEDGMENTS

The authors thank J. M. Chavez and R. A. Soler for their help during the initial characterization of the MgO_x/Au(111) surfaces. The research done at the Chemistry Division of Brookhaven National Laboratory was supported by the U.S. Department of Energy, Office of Science, Office of Basic Energy Sciences, Chemical Sciences, Geosciences, and Biosciences Division, Catalysis Science Program (Grant No DE-SC0012704). This research used resources of the 23-ID-2 (IOS) beamline of the National Synchrotron Light Source II; a U.S. Department of Energy (DOE) Office of Science User Facility operated for the DOE Office of Science by Brookhaven National Laboratory under Contract No. DE-SC0012704.

REFERENCES

- (1) Wang, Q. R.; Guo, J. P.; Chen, P. The impact of alkali and alkaline earth metals on green ammonia synthesis. *Chem.* **2021**, *7* (12), 3203–3220.
- (2) Lee, Y. L.; Jha, A.; Jang, W. J.; Shim, J. O.; Rode, C. V.; Jeon, B. H.; Bae, J. W.; Roh, H. S. Effect of alkali and alkaline earth metal on Co/CeO catalyst for the water gas shift reaction of waste derived synthesis gas. *Appl. Catal. a-Gen* **2018**, *551*, 63–70.
- (3) Karami, H.; Soltanali, S.; Amanati, M.; Song, W.; Liu, J.; Sharifi, K. The promotion effects of alkaline earth metals on the properties of Cr/ η -Al₂O₃ catalysts for propane dehydrogenation. *Journal of Saudi Chemical Society* **2024**, *28*, 101929.
- (4) Tavizón-Pozos, J. A.; Chavez-Esquivel, G.; Suárez-Toriello, V. A.; Santolalla-Vargas, C. E.; Luévano-Rivas, O. A.; Valdés-Martínez, O. U.; Talavera-López, A.; Rodríguez, J. A. State of Art of Alkaline Earth Metal Oxides Catalysts Used in the Transesterification of Oils for Biodiesel Production. *Energies* **2021**, *14*, 1031.
- (5) Kiskinova, M. P. Poisoning and Promotion in Catalysis Based on Surface Science Concepts and Experiments. *Stud. Surf. Sci. Catal.* **1991**, *70*, v.
- (6) Koel, B. E.; Kim, J. *Handbook of Heterogeneous Catalysis*; Wiley: 2008; pp 1–32.
- (7) Hu, L.; Pinto, D.; Urakawa, A. Catalytic Oxidative Coupling of Methane: Heterogeneous or Homogeneous Reaction? *ACS Sustainable Chem. & Eng.* **2023**, *11*, 10835–10844.
- (8) Arndt, S.; Laugel, G.; Levchenko, S.; Horn, R.; Baerns, M.; Scheffler, M.; Schlögl, R.; Schomäcker, R. A Critical Assessment of Li/MgO-Based Catalysts for the Oxidative Coupling of Methane. *Catal. Rev.* **2011**, *53* (4), 424–514.
- (9) Zuo, Z.; Liu, S.; Wang, Z.; Liu, C.; Huang, W.; Huang, J.; Liu, P. Dry Reforming of Methane on Single-Site Ni/MgO Catalysts: Importance of Site Confinement. *ACS Catal.* **2018**, *8*, 9821–9835.
- (10) Pal, R. S.; Rana, S.; Sadhu, S.; Khan, T. S.; Poddar, M. K.; Singha, R. K.; Sarkar, S.; Sharma, R.; Bal, R. Highly active and selective Li/MgO catalysts for methane transformation to C₂ hydrocarbons: Experimental and DFT study. *Energy Advances* **2023**, *2* (1), 180–197.
- (11) Reddy, K. P.; Islam, A.; Tian, Y.; Lim, H.; Kim, J.; Kim, D.; Hunt, A.; Waluyo, I.; Rodriguez, J. A. MgO Nanostructures on Cu(111): Understanding Size- and Morphology-Dependent CO₂ Binding and Hydrogenation. *J. Phys. Chem. C* **2024**, *128*, 7149–7158.
- (12) Islam, A.; Huang, E.; Tian, Y.; Ramirez, P. J.; Reddy, K. P.; Lim, H.; White, N.; Hunt, A.; Waluyo, I.; Liu, P.; Rodriguez, J. A. Low-Temperature Activation and Coupling of Methane on MgO Nanostructures Embedded in Cu₂O/Cu(111). *ACS Nano* **2024**, *18*, 28371–28381.
- (13) Pan, Y.; Benedetti, S.; Nilus, N.; Freund, H.-J. Change of the surface electronic structure of Au(111) by a monolayer MgO(001) film. *Phys. Rev. B* **2011**, *84*, No. 075456.
- (14) Nilus, N.; Benedetti, S.; Pan, Y.; Myrach, P.; Noguera, C.; Giordano, L.; Goniakowski, J. Electronic and electrostatic properties of polar oxide nanostructures: MgO(111) islands on Au(111). *Phys. Rev. B* **2012**, *86*, 205410.
- (15) Xu, C. Q.; Que, Y. D.; Zhuang, Y.; Liu, B.; Ma, Y. P.; Wang, K. D.; Xiao, X. D. Manipulating the Edge of a Two-Dimensional MgO Nanoisland. *J. Phys. Chem. C* **2019**, *123*, 19619–19624.
- (16) Pan, Y.; Benedetti, S.; Noguera, C.; Giordano, L.; Goniakowski, J.; Nilus, N. Compensating Edge Polarity: A Means To Alter the Growth Orientation of MgO Nanostructures on Au(111). *J. Phys. Chem. C* **2012**, *116*, 11126–11132.
- (17) Bignardi, L.; Lizzit, D.; Bana, H.; Travaglia, E.; Lacovig, P.; Sanders, C. E.; Dendzik, M.; Michiardi, M.; Bianchi, M.; Ewert, M.; Buß, L.; Falta, J.; Flege, J. I.; Baraldi, A.; Larciprete, R.; Hofmann, P.; Lizzit, S. Growth and structure of singly oriented single-layer tungsten disulfide on Au(111). *Phys. Rev. Materials* **2019**, *3*, No. 014003.
- (18) Saliba, N.; Parker, D. H.; Koel, B. E. Adsorption of oxygen on Au(111) by exposure to ozone. *Surf. Sci.* **1998**, *410*, 270–282.
- (19) Mehar, V.; Kim, J.; Hunt, A.; Waluyo, I.; Rodriguez, J. A. AP-XPS Study of the Reaction of O₂ and CO₂ with Zn-Au(111) Surface Alloys: Activation of O-O/C-O Bonds and the Formation of ZnO. *J. Phys. Chem. C* **2024**, *128*, 13852–13863.
- (20) Freiburger, E. M.; Düll, F.; Wichmann, C.; Bauer, U.; Steinrück, H.-P.; Papp, C. A high-resolution X-ray photoelectron spectroscopy study on the adsorption and reaction of ethylene on Rh(1 1 1). *Chem. Phys. Lett.* **2022**, *797*, 139595.
- (21) Xu, L.; Wu, Z.; Wang, H.; Shi, J.; Li, Z.; Huang, W. Adsorption and Surface Reactions of C₂H₂ and C₂H₄ on Co(0001). *Surf. Sci. Technol.* **2023**, *1*, 5–13.
- (22) Belgued, M.; Pareja, P.; Amariglio, A.; Amariglio, H. Conversion of methane into higher hydrocarbons on platinum. *Nature* **1991**, *352*, 789–790.
- (23) Isaacs, M. A.; Davies-Jones, J.; Davies, P. R.; Guan, S.; Lee, R.; Morgan, D. J.; Palgrave, R. Advanced XPS characterization: XPS-based multi-technique analyses for comprehensive understanding of functional materials. *Materials Chem. Frontiers* **2021**, *5*, 7931–7963.
- (24) Palomino, R. M.; Gutierrez, R. A.; Liu, Z.; Tenney, S.; Grinter, D. C.; Waluyo, I.; Ramirez, P. J.; Rodriguez, J. A.; Senanayake, S. D. Inverse Catalysts for CO Oxidation: Enhanced Oxide-Metal Interactions in MgO/Au(111), CeO₂(111) and TiO₂/Au(111). *ACS Sustainable Chem. Eng.* **2017**, *5*, 10783–10791.
- (25) Pacchioni, G.; Freund, H.-J. Controlling the Charge State of Supported Nanoparticles in Catalysis: Lessons from Model Systems. *Chem. Soc. Rev.* **2018**, *47*, 8474–8502.